J Mater Sci (2010) 45:6611–6616
DOI 10.1007/s10853-010-4751-6

# Synthesis and photocatalytic behaviors of $Cr_2O_3$–CNT/$TiO_2$ composite materials under visible light

**Ming Liang Chen · Kwang Youn Cho · Won Chun Oh**

Received: 13 March 2010 / Accepted: 5 July 2010 / Published online: 17 July 2010


**Abstract** $Cr_2O_3$–CNT/$TiO_2$ composites derived from chromium acetylacetonate, multi-walled carbon nanotubes (MWCNT) and titanium *n*-butoxide (TNB) were prepared, and the photocatalytic activity of the $Cr_2O_3$–CNT and CNT/$TiO_2$ composites was examined. The $Cr_2O_3$–CNT/$TiO_2$ composites were characterized by BET surface area measurement, X-ray diffraction, transmission electron microscopy, and energy dispersive X-ray analysis. The photocatalytic activity was determined from the decomposition of methylene blue (MB) under visible light irradiation. Methylene blue was photodegraded successfully in the presence of the $Cr_2O_3$–CNT/$TiO_2$ composite under visible light irradiation.

## Introduction

Metal oxide photocatalysts have attracted increasing attention for their possible applications to the degradation of environmental organic pollutants and solar-energy conversion [1–6]. $TiO_2$ is one of the most important semiconducting oxides owing to its photocatalytic activity, conservative nature, low cost, low toxicity, and stable to light illumination. In addition to these properties, its ability to photocatalytic decompose organic materials has been applied in the environmental industry, i.e., organic pollutant treatment [7, 8]. Anatase has higher photocatalytic activity and has been studied more than the other two forms of $TiO_2$ [9]. However, the wide band gap (3.2 eV) and high electron–hole recombination rate of $TiO_2$ limits its use [10]. $TiO_2$ only strongly absorbs UV light ($\lambda$ <380 nm), which accounts for a small fraction of the solar spectrum (<4%). Therefore, the development of modified $TiO_2$ with high activity under visible light ($\lambda$ >380 nm) is needed take full advantage of the main part of the solar spectrum (mostly 400–600 nm) and even the poor illumination of interior lighting.

Therefore, many studies have been carried out to convert the $TiO_2$ absorption from the ultraviolet to visible light region by the ion doping of transition metals [11]. The presence of metal ion dopants in $TiO_2$ crystal lattice affects its photoreactivity by altering the charge carrier recombination and interfacial electron-transfer rates by shifting the band gap of the catalysts to the visible region [12]. A dopant ion may act as an electron trap or hole trap. This would prolong the lifetime of the generated charge carriers, resulting in enhanced photocatalytic activity [13]. Among these transition metal ions, $Cr^{3+}$ has attracted considerable attention because its introduction can extend the visible light absorption.

On the other hand, carbon nanotubes (CNTs)-based composites have attracted considerable attention owing to their unique electrical and structural properties. CNTs exhibit good electron conductivity, high surface area, and high adsorption capacities. Recently, CNTs were reported to be a promising material for use in environmental cleaning. Meanwhile, with the development of preparation technology, the price of CNTs has decreased significantly, and it is possible for CNTs to be used in a large-scale operations. CNTs can conduct $e^-$ and have a high adsorption capacity. Therefore, they can be considered

M. L. Chen · W. C. Oh (✉)
Department of Advanced Materials and Science Engineering, Hanseo University, Seosan-si, Chungnam-do 356-706, Korea
e-mail: wc_oh@hanseo.ac.kr

K. Y. Cho
Korea Institute of Ceramic Engineering and Technology, Seoul 153-801, Korea

excellent dopants and supports for $TiO_2$-based materials for use as photocatalysts. From previous studies [14, 15], CNTs may accept a photo-induced electron ($e^-$) by UV irradiation in the CNT/$TiO_2$ composite, so it can act as electron sensitizer and donator. Therefore, the photocatalytic efficiency can be improved by increasing the number of electrons.

In this study, chromium acetylacetonate {$Cr(C_5H_7O_2)_3$}, multi-walled carbon nanotubes (MWCNT), and titanium *n*-butoxide (TNB, $Ti(OC_4H_7)_4$) were used to prepare $Cr_2O_3$–CNT catalysts and $Cr_2O_3$–CNT/$TiO_2$ composites. Their properties were examined by the BET surface area, X-ray diffraction (XRD), transmission electron microscopy (TEM), and energy dispersive X-ray analysis (EDX). Their photocatalytic activity under visible light was determined from the decomposition of methylene blue (MB) in an aqueous solution. The effect of the transition metal (Cr) on the photocatalytic degradation of the MB solution was examined by comparing the photocatalytic activity of the $Cr_2O_3$–CNT/$TiO_2$ composites with that of the CNT–$TiO_2$ composites prepared in a previous study [16].

## Experimental

### Materials

Crystalline MWCNT powder (95.9 wt%, Carbon Nanomaterial Technology Co., Ltd, Korea), 20 nm in diameter and 5 μm in length, was used as the starting material. Chromium acetylacetonate {97%, $Cr(C_5H_7O_2)_3$, Sigma–Aldrich Chemistry, USA} was used as the transition metal (Cr) precursor. Titanium *n*-butoxide (TNB, $Ti(OC_4H_7)_4$), Acros organics Co., Ltd, USA) was used as the $TiO_2$ precursor. *m*-Chlorperbenzoic acid (MCPBA, Acros Organics, New Jersey, USA) was used to oxidize the MWCNT. Benzene (99.5%, Samchun Pure Chemical Co., Ltd, Korea) was used as the solvent. Methylene blue (MB, $C_{16}H_{18}N_3S\cdot Cl\cdot 3H_2O$, Dukan Pure Chemical Co., Ltd, Korea), of analytical grade, was selected because it can readily produce potentially more hazardous aromatic amines under anaerobic conditions.

### Synthesis of $Cr_2O_3$–CNT and $Cr_2O_3$–CNT/$TiO_2$ composites

Before preparing the $Cr_2O_3$–CNT and $Cr_2O_3$–CNT/$TiO_2$ composites, the surface of the MWCNT should be oxidized by strong acids to introduce active function groups. According to a previous study [14], 1.0 g of MCPBA dissolved in 60 mL benzene was used as the oxidizing agent. Subsequently, 0.5 g MWCNT was added to the oxidizing agent. The mixture was stirred with a magnetic stirrer for 6 h at 343 K. The MWCNT were dried at 373 K and stored until needed.

Chromium acetylacetonate was dissolved in benzene to prepare the 0.01 M chromium solution. A certain amount of oxidized MWCNT was placed into a certain volume of a chromium solution. The solution was the homogenized at 343 K for 5 h using a shaking water bath (Lab house, Korea) at a shaking rate of 120 rpm/min. After a reaction for 5 h, the solution was transformed to a $Cr_2O_3$–CNT gel, which was heat treated at 873 K for 1 h at a heating rate of 279 K/min to prepare the $Cr_2O_3$–CNT composite.

In a separate preparation, TNB (4 mL) was dissolved in 46 mL of benzene with constant stirring to form a TNB-benzene solution. The prepared $Cr_2O_3$–CNT composite was placed into this solution. The mixture was then reacted at 343 K for 5 h using a shaking water bath at a shaking rate of 120 rpm/min. After this reaction, the mixture was treated thermally at 873 K for 1 h at a heating rate of 279 K/min. Finally, the $Cr_2O_3$–CNT/$TiO_2$ composite was obtained.

### Characterization

The synthesized $Cr_2O_3$–CNT and $Cr_2O_3$–CNT/$TiO_2$ composites were characterized using a variety of techniques. The BET surface area was measured using a Quantachrome surface area analyzer (Monosorb, USA). XRD was used for crystal phase identification and to estimate the anatase-to-rutile ratio. The XRD patterns were obtained at room temperature with a Shimata XD-D1 (Japan) apparatus using CuKα radiation. TEM (JSM-5200 JOEL, Japan) was used to observe the surface state and structure of the $Cr_2O_3$–CNT and $Cr_2O_3$–CNT/$TiO_2$ composites. EDX was used to measure the elemental analysis of the $Cr_2O_3$–CNT and $Cr_2O_3$–CNT/$TiO_2$ composites. The light absorption spectra of the samples were recorded using a UV–vis spectrophotometer (Optizen POP, Mecasys Co., Ltd, Korea) over the 200–750 nm range.

### Photocatalytic activity

The photocatalytic activity of the $Cr_2O_3$–CNT and $Cr_2O_3$–CNT/$TiO_2$ composites was examined from the decomposition of a MB solution under visible light irradiation. In an ordinary photocatalytic test performed at 25 °C, 0.05 g of the composite was added to 50 mL of a $1.0 \times 10^{-5}$ mol/L MB solution and maintained in suspension by magnetic stirring. After stirring continuously in the dark for 2 h to ensure the establishment of adsorption/desorption equilibrium of MB, the suspension was irradiated with visible light (8 W, $\lambda$ >420 nm, KLD-08L/P/N, Fawoo Technology) and treated as the starting point ($t = 0$) of the reaction, where the concentration of MB was designated as $c_0$.

At specific time (30 min, 60 min, 90 min, and 120 min) intervals, a certain volume of the sample was withdrawn and centrifuged to remove the catalyst prior to analysis. The concentration of the MB ($c$) solution during the photocatalytic degradation reaction was monitored by measuring the absorbance of the solution samples using a UV–vis spectrophotometer at $\lambda_{max} = 660$ nm.

## Results and discussion

### Characterization

Table 1 shows the BET surface area of pristine MWCNT, $Cr_2O_3$–CNT, $Cr_2O_3$–CNT/$TiO_2$, and CNT/$TiO_2$ composites. The surface area of the pristine MWCNT and $Cr_2O_3$–CNT composite was 299 and 278 $m^2$/g, respectively. However, the surface area of the $Cr_2O_3$–CNT/$TiO_2$ composite was considerably lower, 47 $m^2$/g. Moreover, the surface area of the CNT/$TiO_2$ composite was also smaller than that of pristine MWCNT, 84 $m^2$/g. It appears that the metal oxide was dispersed over the surface of the MWCNT, which can congest the pores of the MWCNT, and decrease the surface area. It is believed that the surface area decreased with increasing amount of metal oxide in the composites, which is supported by EDX elemental microanalysis.

The metal components in the materials were estimated from the XRD patterns. Figure 1 shows the XRD patterns of $Cr_2O_3$–CNT, $Cr_2O_3$–CNT/$TiO_2$, and CNT/$TiO_2$ composites calcined at 873 K. In the $Cr_2O_3$–CNT composite, the peaks at 36° and 44° 2$\theta$ due to $Cr_2O_3$ (JCPDS, No. 38-1479) [17] and peaks at 27° 2$\theta$ due to graphite (JCPDS, No. 26-1080) were observed [18]. The $Cr_2O_3$–CNT/$TiO_2$ composite showed peaks at 24°, 34°, 36°, 42°, and 50° 2$\theta$ due to $Cr_2O_3$ (JCPDS, No. 38-1479) [17] and peaks at 25°, 37°, 48°, and 54° 2$\theta$ due to anatase $TiO_2$ (JCPDS, No. 21-1272) [19]. The CNT/$TiO_2$ composite also showed characteristic peaks for anatase $TiO_2$. However, the XRD peaks for the C component were not clearly observed in the $Cr_2O_3$–CNT/$TiO_2$ and CNT/$TiO_2$ composites due to its amorphous structure and lower C content.

**Table 1** The BET surface area of pristine MWCNTs, $Cr_2O_3$–CNT, $Cr_2O_3$–CNT/$TiO_2$ and CNT/$TiO_2$ composites

| Samples | $S_{BET}$ ($m^2$/g) |
|---|---|
| Pristine MWCNT | 299 |
| $Cr_2O_3$–CNT | 278 |
| $Cr_2O_3$–CNT/$TiO_2$ | 47 |
| CNT/$TiO_2$ | 84 |

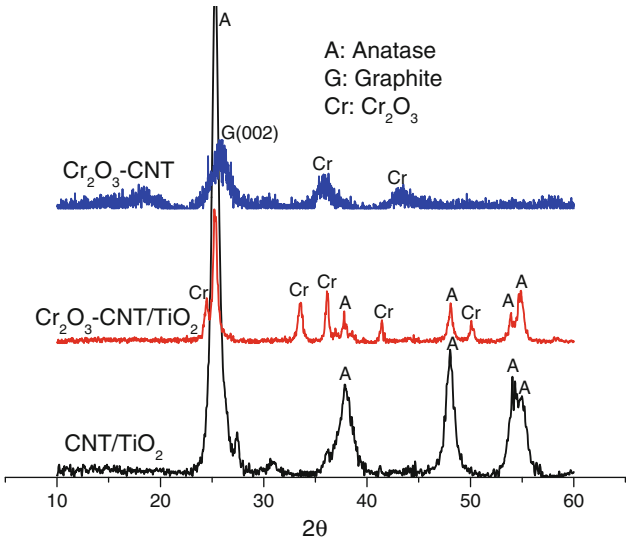


**Fig. 1** The XRD patterns of $Cr_2O_3$–CNT, $Cr_2O_3$–CNT/$TiO_2$, and CNT/$TiO_2$ composites

TEM images of the $Cr_2O_3$–CNT, $Cr_2O_3$–CNT/$TiO_2$, and CNT/$TiO_2$ composites were examined to determine the dispersion states and sizes of the metal oxide particles in the composites. Figure 2 shows TEM images of $Cr_2O_3$–CNT, $Cr_2O_3$–CNT/$TiO_2$, and CNT/$TiO_2$ composites. The $Cr_2O_3$–CNT composite (Fig. 2a) contained $Cr_2O_3$ particles, 10–15 nm in diameter, dispersed uniformly and homogenously over the surface of the MWCNT. $Cr_2O_3$–CNT/$TiO_2$ composite (Fig. 2b) showed the presence of either deep-color particles, possibly $Cr_2O_3$, or rather light-colored particles, approximately 20 nm size, possibly $TiO_2$. In addition, the $Cr_2O_3$ and $TiO_2$ particles were distributed homogenously over the surface of the MWCNT. This suggests that the calcined materials were composed of nano-sized $Cr_2O_3$ and $TiO_2$ particles over the surface of MWCNT. This structure would show excellent photocatalytic activity. The CNT/$TiO_2$ composite (Fig. 2c) showed $TiO_2$ particles dispersed over the surface of the MWCNT with some agglomeration.

EDX microanalysis was carried out to determine the elemental composition. Table 2 lists the main elements and wt% of each element in $Cr_2O_3$–CNT, $Cr_2O_3$–CNT/$TiO_2$, and CNT/$TiO_2$ composites. All the composites contained C, indicating that the MWCNT were present after introducing the metal oxides and heat-treatment. With the exception of C, the $Cr_2O_3$–CNT composite contained Cr and O, indicating the presence of $Cr_2O_3$. CNT/$TiO_2$ composite contained Ti and O, indicating $TiO_2$. The $Cr_2O_3$–CNT/$TiO_2$ composite contained Ti, Cr, and O element, indicating the co-existence of $Cr_2O_3$ and $TiO_2$.

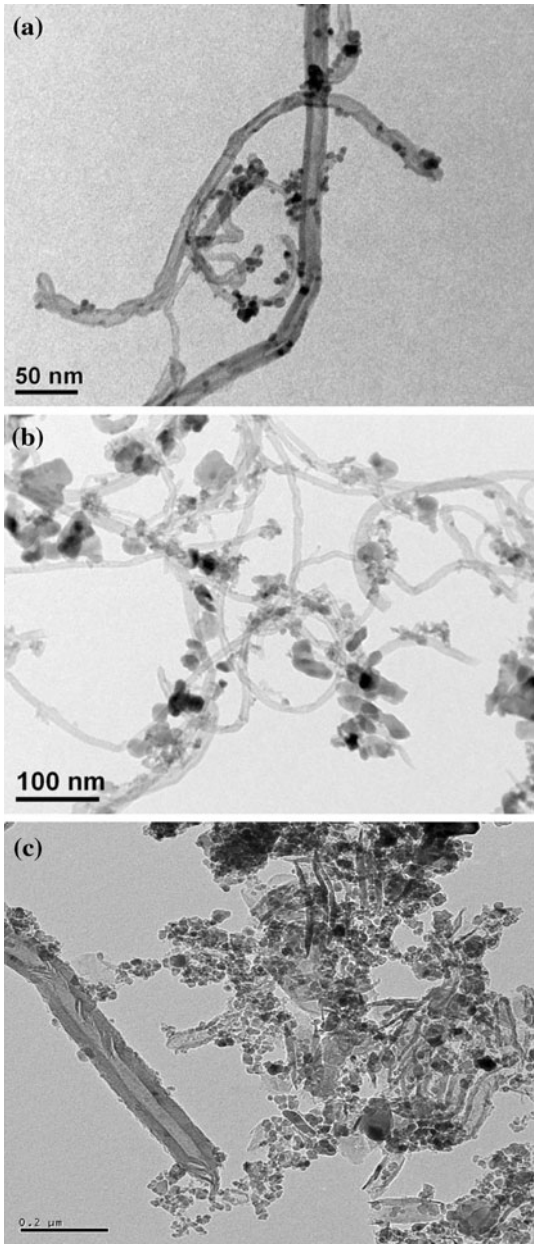


**Fig. 2** TEM images of $Cr_2O_3$-CNT (**a**), $Cr_2O_3$-CNT/$TiO_2$ (**b**), and CNT/$TiO_2$ (**c**) composites

**Table 2** EDX elemental microanalysis (wt%) of $Cr_2O_3$–CNT, $Cr_2O_3$–CNT/$TiO_2$, and CNT/$TiO_2$ composites

| Samples | Elements | | | |
|---|---|---|---|---|
| | C | O | Ti | Cr |
| $Cr_2O_3$–CNT | 68.89 | 10.93 | – | 20.18 |
| $Cr_2O_3$–CNT/$TiO_2$ | 24.21 | 39.15 | 17.77 | 18.87 |
| CNT/$TiO_2$ | 25.42 | 34.76 | 39.82 | – |

## Degradation effects of MB solution

### *Adsorption degradation of MB solution*

As mentioned in the "Experimental" section, the MB solution mixed with the composites was kept in the dark with constant stirring for 2 h, which belongs to the adsorption degradation stage. At this time, the concentration of the MB solution was designated as $c_0$, which can describe the adsorption degradation effect of each composite. Figure 3 shows the % MB removal over the $Cr_2O_3$–CNT, $Cr_2O_3$–CNT/$TiO_2$, and CNT/$TiO_2$ composites after stirring at the dark for 2 h, and turning on visible light. The $Cr_2O_3$–CNT composite showed highest MB removal efficiency, which reached 68%. The CNT/$TiO_2$ and $Cr_2O_3$–CNT/$TiO_2$ composite had a MB removal efficiency of 40% and 30%, respectively. The BET surface area has a significant effect on adsorption degradation. A larger surface area has higher adsorption ability. According to the BET surface area, the $Cr_2O_3$–CNT composite has a much larger surface area than the CNT/$TiO_2$ and $Cr_2O_3$–CNT/$TiO_2$ composite. Therefore, the $Cr_2O_3$–CNT composite has the largest adsorption ability of the three composites examined.

### *Photocatalytic degradation of MB solution*

Photocatalytic degradation began after turning on the visible lamp. The concentration of the MB solution was analyzed at specific times (30, 60, 90, and 120 min) to determine the photocatalytic degradation efficiency for each composite.

The degradation efficiency ($\varphi$) was calculated using the following equation:

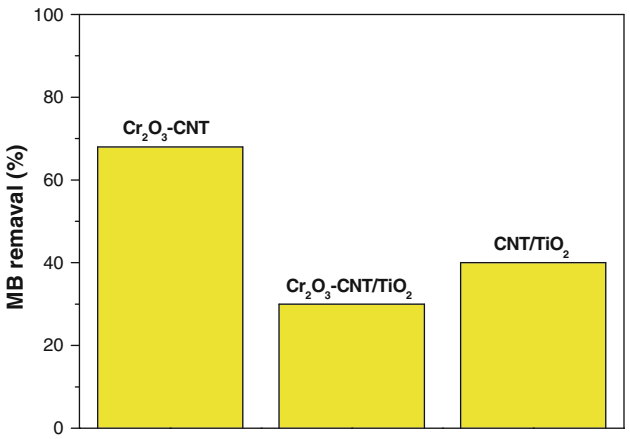


**Fig. 3** MB removal by adsorption degradation for $Cr_2O_3$–CNT, $Cr_2O_3$–CNT/$TiO_2$, and CNT/$TiO_2$ composites after stirring in dark for 2 h

$$\varphi = (c - c_0)/c \times 100 \quad (1)$$

where $\varphi$ is the degradation efficiency of the MB solution, $c_0$ is the initial dye concentration, and $c$ is the dye concentration after degradation.

The photocatalytic degradation of the MB solution followed the first-order decay kinetics [20]. Previous studies reported that the photocatalytic degradation rate of textile dyes in heterogeneous photocatalytic oxidation systems under UV-light illumination followed the Langmuir–Hinshelwood (L–H) kinetics model.

$$r = \mathrm{d}c/\mathrm{d}t = kKc/(1 + Kc) \quad (2)$$

where $r$ is the oxidation rate, $c$ is the concentration of the reactant, $t$ is the illumination time, $k$ is the reaction rate constant, and $K$ is the adsorption coefficient of the reactant. At low initial dye concentrations ($c_0$ small), the rate was proportional to the dye concentration and the rate constant was observed to be a pseudo-first-order constant [21]. Accordingly, Eq. 2 can be changed to Eq. 3.

$$-\ln(c/c_0) = kKt = k_{\mathrm{app}}t \quad (3)$$

Figure 4 shows the apparent first-order linear transform $-\ln(c/c_0)$ as a function of $f(t)$ of the MB degradation kinetic plots for pure $TiO_2$, $Cr_2O_3$–CNT, $Cr_2O_3$–CNT/$TiO_2$, and CNT/$TiO_2$ composites under visible light irradiation. The plot of $-\ln(c/c_0)$ versus time in Fig. 4 produces a straight line from which the slope of the linear variations equals the apparent first-order rate constant, $k_{\mathrm{app}}$.

The concentration of the MB solution decreased with increasing irradiation time of visible light for all composites. In addition, the apparent first-order rate constant ($k_{\mathrm{app}}$) for pure $TiO_2$, CNT/$TiO_2$, $Cr_2O_3$–CNT, and $Cr_2O_3$–CNT/$TiO_2$ composites was $3.0 \times 10^{-4}$ min$^{-1}$, $9.8 \times 10^{-4}$ min$^{-1}$, $2.2 \times 10^{-3}$ min$^{-1}$, and $4.41 \times 10^{-3}$ min$^{-1}$, respectively. This suggests that pure $TiO_2$ has almost no photocatalytic activity for the MB solution under visible light irradiation, whereas the CNT/$TiO_2$ composite exhibited a small amount of photocatalytic activity. However, the $Cr_2O_3$–CNT composite has a relative larger photocatalytic activity for the MB solution under visible light, which indicates that $Cr_2O_3$ has photocatalytic activity under visible light. Moreover, the $Cr_2O_3$–CNT/$TiO_2$ composite showed the best photodegradation efficiency for MB solution under visible light irradiation.

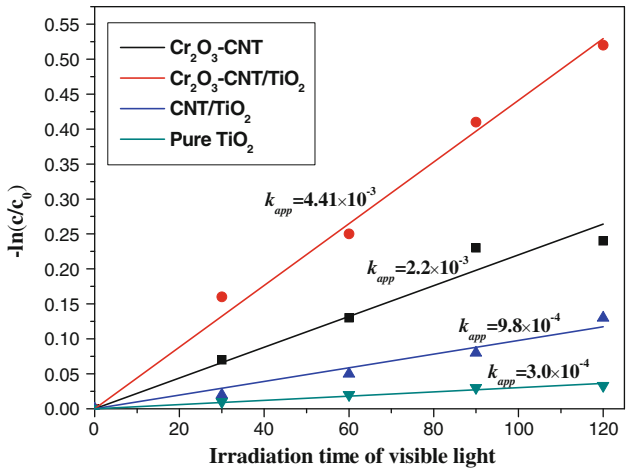


**Fig. 4** Apparent first-order linear transform $-\ln(c/c_0)$ against $f(t)$ of MB degradation kinetic plots for pure $TiO_2$, $Cr_2O_3$–CNT, $Cr_2O_3$–CNT/$TiO_2$, and CNT/$TiO_2$ composites under the visible light irradiation

The photocatalytic activity of $TiO_2$ can be controlled by the following factors: (i) light absorption wavelength; (ii) rate of the electron or hole induced redox reaction; and (iii) recombination of the electron–hole. When a transition metal ion ($Cr^{3+}$) is incorporated into the $TiO_2$ lattice, the dopant level appears between the valence band and conduction band of $TiO_2$ [22], thereby altering the band-gap energy and shifting the absorbance edge to the visible light region. According to previous studies [23], MWCNT can act as an electron sensitizer and donor in the composite photocatalyst to accept a photo-induced electron ($e^-$) into the conduction band of $TiO_2$ particles under light irradiation, thereby increasing the number of electrons as well as the rate of electron-induced redox reactions. The addition of a transition metal also has a charge trapping effect. Charge trapping can be demonstrated by the following equations [24]:

$$TiO_2 + h\nu \rightarrow e^-_{cb} + h^+_{vb} \quad (4)$$

$$M^{n+} + e^-_{cb} \rightarrow M^{(n-1)+} \quad (5)$$

$$M^{n+} + h^+_{vb} \rightarrow M^{(n+1)+} \quad (6)$$

The holes can transfer to the $TiO_2$ surface and react with $OH^-$ to produce active OH·. When a transition metal ion replaces Ti ions in the $TiO_2$ lattice, most of the dopant levels appeared between the valence band and conduction band of $TiO_2$. This can increase the surface trapping rate of the carrier and retard the electron–hole recombination [10] as well as enhance the photocatalytic activity of $TiO_2$. Consequently, the photodegradation of the MB solution on the $Cr_2O_3$–CNT/$TiO_2$ composite would be caused by the two types of photocatalysts, $TiO_2$ and $Cr_2O_3$. As described above, only three factors were modified to enhance the photocatalytic activity. However, all three factors could be modified using the $Cr_2O_3$–CNT/$TiO_2$ composite. Therefore, this composite showed the best photodegradation efficiency for the MB solution under visible light irradiation among the three composites examined.

## Conclusions

This paper reports the preparation and characterization of $Cr_2O_3$–CNT and $Cr_2O_3$–CNT/$TiO_2$ composites, as well as a comparison of their photocatalytic activity with a CNT/$TiO_2$ composite prepared in previous work. The BET surface area of the $Cr_2O_3$–CNT/$TiO_2$ composite was significantly lower than that of the pristine MWCNT. XRD revealed both $Cr_2O_3$ and anatase $TiO_2$ in the $Cr_2O_3$–CNT/$TiO_2$ composite. However, the peaks for C could not be seen clearly in $Cr_2O_3$–CNT/$TiO_2$ due to its amorphous structure and low C content. From the TEM images, the $Cr_2O_3$ and $TiO_2$ particles were distributed homogenously on the surface of the MWCNT for $Cr_2O_3$–CNT/$TiO_2$ composite. EDX showed that $Cr_2O_3$–CNT/$TiO_2$ composite contained C, Ti, Cr, and O. The Cr ions in the $TiO_2$ structure caused a significant absorption shift into the visible region, the MWCNTs accepted the photo-induced electron ($e^-$) under visible light irradiation to increase the amount of electrons, and the Cr ions could increase the surface trapping rate of the carrier and retard electron–hole recombination. Therefore, the photodegradation of the MB solution for the $Cr_2O_3$–CNT/$TiO_2$ composite could be caused by two types of photocatalysts, $TiO_2$ and $Cr_2O_3$, and it had the best photodegradation efficiency for the MB solution under visible light irradiation among the three composites examined.

## References


1. Fujishima A, Honda K (1972) Nature 238:37
2. Mills A, Hunte SL (1997) J Photochem Photobiol A 108:1
3. Tryk DA, Fujishima A, Honda K (2000) Electrochim Acta 45:2363
4. Hoffmann MR, Martin ST, Choi W, Bahnemann DW (1995) Chem Rev 95:69
5. Zou Z, Ye J, Sayama K, Arakawa H (2001) Nature 414:625
6. Hagfeldt A, Gŕatzel M (2000) Acc Chem Res 33:269
7. Sivalingam G, Nagaveni K, Hegde MS, Madras G (2003) Appl Catal B 45:23
8. Mohapatra P, Parida KM (2006) J Mol Catal A 258:118
9. Barakat MA, Schaeffer H, Hayes G, Ismat-Shah S (2005) Appl Catal B 57:23
10. Colmenares JC, Aramendia MA, Marinas A, Marinas JM, Urbano FJ (2006) Appl Catal A 306:120
11. Karvinen S (2003) Solid State Sci 5:811
12. Ji-Chuan X, Yan-Li S, Huang JE, Wang B, Hu-Lin L (2004) J Mol Catal A 219:351
13. Choi W, Termin A, Hoffmann MR (1994) Angew Chem Int Ed Engl 33:1091
14. Oh WC, Chen ML (2008) Bull Korean Chem Soc 29:159
15. Chen ML, Oh WC (2008) Anal Sci Technol 21:229
16. Oh WC, Zhang FJ, Chen ML (2009) Bull Korean Chem Soc 30:2637
17. Miyazaki H, Matsui H, Nagano T, Karuppuchamy S, Ito S, Yoshihara M (2008) Appl Surf Sci 254:7365
18. Oh WC, Zhang FJ, Chen ML (2010) J Ind Eng Chem 16:321
19. Chen ML, Bae JS, Oh WC (2006) Anal Sci Technol 19:460
20. Ghasemi S, Rahimnejad S, Rahman Setayesh S, Hosseini M, Gholami MR (2009) Prog React Kinet Mech 34:55
21. Oh WC, Zhang FJ, Chen ML (2010) J Ind Eng Chem 16:299
22. Dong YL, Won JL, Jae Sung S, Jung HK, Yang SK (2004) Comput Mater Sci 30:383
23. Chen ML, Zhang FJ, Oh WC (2009) New Carbon Mater 24:159
24. Choi W, Termin A, Hoffmann MR (1994) J Phys Chem 98:13669